A Numerical Study on Agglomeration in High Temperature Fluidized beds

Zahra Mansourpour[*], **Navid Mostoufi and Rahmat Sotudeh-Gharebagh**
School of Chemical Engineering, College of Engineering, University of Tehran, Tehran, Iran

Abstract

Soft-sphere discrete element method (DEM) and Navier-Stokes equations were coupled with equations of energy for gas and solids to investigate the process of agglomeration in fluidized bed of polyethylene particles at high temperature. The Newton's second law of motion was adapted for translational and rotational motion of particles and agglomerates. The cohesive force for polyethylene particles was calculated based on a time dependent model for solid bridging by the viscous flow mechanism. The motion of agglomerates was described by means of the multi-sphere method. By taking into account the cohesiveness of particles at high temperatures and considering real dynamic agglomerates, the fluidization behavior of a bed of polyethylene particles was successfully simulated in terms of increasing the size of agglomerates. Effect of the inlet gas temperature on mass and size of agglomerates was investigated. A mechanistic study in terms of contact time, cohesive force and repulsive force, which are the key parameters in the formation of agglomerates, were also carried out.

Introduction

In high temperature fluidized beds, such as gas-phase polymerization reactors and iron oxide reduction beds, formation of agglomerates via solid bridge is a well-recognized feature. In order to use these types of reactors more effectively, there is a need to obtain a fundamental understanding of the dynamic behavior of such systems. Fortunately recent progress in the computational resources, have allowed carrying out detailed simulations of different aspects of the complex phenomena occurring in the fluidized beds. Popular mathematical models proposed thus far can be grouped into two categories: the continuum-continuum approach at a macroscopic level represented by the so called two fluid model (TFM) [1] and continuum–discrete approach at a macroscopic level mainly represented by the so called combined computational fluid dynamics and discrete element method (CFD-DEM) [2]. In the CFD-DEM, the motion of particles is modeled as a discrete phase, described by the Newton's second law of motion for an individual particle, while the flow of fluid (gas or liquid) is treated as a continuum phase, described by the local averaged Navier-Stokes equation in a computational cell. This method has been recognized as an effective method to study the fundamentals of particle-fluid flow at different conditions [3]. Although several investigations have been conducted to simulate the behavior of agglomerating fluidized beds with wet particles by considering cohesive force as a result of liquid bridge [4] and particles with van der Waals force interaction [5] based on the DEM, a few reports exist about simulation of the whole mechanism of agglomeration in fluidized beds at high temperatures. Li et al. [6] reviewed recent advantage in the DEM for describing motion, deposition, agglomeration or aggregation of a large number of adhesive spherical particles including van der Waals force, ligand-receptor binding, liquid bridging force, interface adhesion, and sintering forces. Kuwagi et al. [7] developed a model for metallic solid bridge by surface diffusion mechanism including the effect of surface roughness by CFD-DEM simulation. In their model, the sintering phenomenon occurs between contacting particles of the same temperature. Moreover, agglomerates

---
[*] Corresponding author: Tel: +98- 21- 61112196   Email: mansourp@ut.ac.ir

were defined as clusters of primary particles in which solid bridges sustain during the collision of particles. The formed agglomerates move only with the translational motion. The most important issue that can be detected by this definition is early de-fluidization of the bed. When particles stick to each other, both translational and rotational motions provide the real mobility of the fluidized bed. Omitting the rotational motion of agglomerates and considering the same temperature for particles lead to sudden de-fluidization of the bed in the model developed by Kuwagi et al. [7]. Therefore, the possibility of studying macroscopic behavior of particulate systems, which is controlled by interaction forces, is limited in this condition. Mansourpour et al. [8, 9] proposed a new approach according to the multi-sphere method based on the CFD-DEM to explore the agglomeration phenomena in a fluidized bed. The effect of operating condition including pressure and velocity on agglomeration state was investigated in macro and micro- scale studies.

In the present work, it was tried to define the sintered agglomerate as a real object in which its translational and rotational motions are calculated according to the multi-sphere method based on the CFD-DEM and investigate the effect of inlet temperature on the fluidization state. In the previous work [7] in which the effect of inlet temperature on the fluidization was considered, the motion of agglomerates and particles were described by translational motion rather than both translational and rotational motions which are the realistic description of object's motion according to the laws of dynamics. Considering just the translational motion of agglomerates, results in the sudden de-fluidization of bed. But de-fluidization proceeds gradually when the motions of agglomerates are described based on both rotational and translational motions. The model was completed with applying energy balance equations for both gas and particles in order to consider

temperature distribution effect on agglomeration behavior. Formation of solid bridge between contacting particles was modeled by the viscose flow mechanism. The variation of the mass and the size of agglomerates were investigated at the various inlet gas temperatures.

2. Model developments

The CFD-DEM code used for the present work was developed in our previous work [10]. In this model, the gas phase was described with the volume-averaged Navier-Stokes equation. The Newton's second law of motion was adapted for translational and rotational motion of particles and agglomerates at any time t as follows:

$$m\frac{d\vec{V_i}}{dt}=\sum_{j=1}^{k_i}(\vec{f}_{cont,n,i,j}+\vec{f}_{cont,t,i,j})+\vec{f}_{f,i}+\vec{f}_{g,i}+\vec{f}_{coh} \quad (1)$$

$$I_i\frac{d\omega_i}{dt}=\sum_{j=1}^{k_i}\vec{R}_{i,j}\times\vec{f}_{cont,t,i,j} \quad (2)$$

In the agglomeration phenomenon, particles adhere to each other via solid bridge and form larger agglomerates. Since agglomerates with irregular shapes are formed during the agglomeration process, it was required to adapt an appropriate model to track them as a real object. As the agglomerate is a collection of spherical particles which can retain their solid bridge with no overlap, the motion of agglomerates can be described according to the multi-sphere method proposed by Kruggel-Emden et al. [11]. The cohesive force (f_{coh}) was calculated based on a time dependent model proposed by Seville et al. [12] for solid bridging by viscous flow mechanism for polyethylene (PE) particles at high temperature. When the temperature of a particle increases to higher than the softening point of PE (95 ^{0}C), the particle surface becomes sticky. Colliding particles with sticky surface grow towards larger agglomerates due to formation of permanent solid bridges.

The procedure of solid bridge formation between colliding particles is as follows:

a) In each time step, when it is found that two particles have newly come into contact, the contact time (t_{con}) corresponding to their inter-particle solid bridge is stored. The radius of solid bridge increases during the contact time with respect to the temperature of colliding particles according to the following formula [12]:

$$x_{s.b.} = (\frac{3\gamma_p r t_{con}}{2\mu_p})^{1/2} \qquad (3)$$

The rate of material migration to the contact point is a sensitive function of temperature in the viscous flow mechanism. The sintering is opposed by viscosity which has the Arrhenius type function of temperature:

$$\mu_p = \mu_0 \exp(\frac{E_s}{RT}) \qquad (4)$$

The solid bridge force is then expressed as follows:

$$f_{coh.} = \pi x_{s.b.}^2 \sigma_{s.b.} \qquad (5)$$

b) In each time step, there are two possibilities for particles that were previously in contact:
b-1) If they are still in contact, their contact time is modified as:

$$t_{con.} = t_{con.,0} + \Delta t \qquad (6)$$

and the solid bridge force is calculated according to Eqs. (3) –(5) in this time step.
b-2) If the deformation period is finished and particles are not in contact anymore, the solid bridge is examined whether it can remain or not. The solid bridge strength can be judged by the maximum repulsion force ($f_{rep,max}$) during deformation. The value of $f_{rep,max}$ can be calculated according to the maximum deformation during the contact period by the following equation:

$$f_{rep,max} = k_n \delta_{max} \qquad (7)$$

If $f_{rep,max} > f_{coh}$ the solid bridge breakage takes place but if $f_{rep,max} < f_{coh}$ the solid bridge remains firm between the two colliding particles and they are sintered and remain in the same agglomerate.

c) In each time step, when the solid bridge between two particle is broken in a collision, $x_{s.b.}$ and t_{con} are set to zero.
The velocity of any agglomerate formed from sticking individual particles, particle and an agglomerate or two agglomerates is calculated according to the momentum conservation before and after the collision.
Since the solid bridging is a time dependent mechanism, incorporating the agglomeration model into the CFD-DEM approach is possible via the soft sphere approach. Equations used to calculate the fluid-particle force and contact forces between the particles in this work are listed in Table 1. Equations of energy balance were considered for both gas and particle phases. More details about the trajectory of gas and solid phase coupling and strategy of solving are described by Mansourpour et al. [10].

3. Results and discussion
3.1. Case study
To explore the agglomeration phenomenon in a gas-solid fluidized bed, a set of numerical simulations were conducted. Table 2 summarizes the computational conditions and parameters used in these simulations. The coefficients of restitution and friction for PE particles were considered as 0.9 and 0.3, respectively. The bed was rectangular with 0.06 m width, 0.24 m height and initially filled with 5000 particles. The thickness of the bed was 0.001 m (equal to the diameter of large particles). The packing condition was achieved by randomly positioning the particles in the bed and allowing them to settle by their gravitational force for one second (without cohesive force) which formed a packed bed with 0.06 m height. At this stage, the hot gas was injected into the bed through the uniform distributor considered for this bed. Initial temperature of particles and inlet gas temperature were 95 ^{0}C and 110 ^{0}C, respectively. Different operating temperatures, ranging from 100 ^{0}C to 130 ^{0}C, were used in simulations. The parameters attributed to the polyethylene

and viscous flow mechanism was considered based on the experimental data reported by Seville et al. [13].

Table 1: Details of expressions used for calculating contact and drag forces acting on particle i

Forces or torque		Symbol	Equation
Normal forces	Contact	$\vec{f}_{cn,ij}$	$-(k_n\delta_{c,ij})\vec{n}_i$
	Damping	$\vec{f}_{dn,ij}$	$-(\eta_i\vec{V}_{r,ij}.\vec{n}_i)\vec{n}_i$
Tangential forces	Contact	$\vec{f}_{ct,ij}$	$-\left(\min\left(\mu\left|\vec{f}_{cn,ij}\right|,\left|k_t\delta_{t,ij}\vec{t}_i\right|\right)\dfrac{\delta_{t,ij}}{\left|\delta_{t,ij}\right|}\right)\vec{t}_i$
	Damping	$\vec{f}_{dt,ij}$	$-\eta_i\left[\left(\vec{V}_{r,ij}.\vec{t}_i\right)+\left(\vec{\omega}_i\times\vec{R}_i-\vec{\omega}_j\times\vec{R}_j\right)\right]$
Torque	Interparticle	$\vec{T}_{i,j}$	$\vec{R}_i\times\vec{f}_{c,ij}$
Gravity		$\vec{f}_{g,i}$	$m_i\vec{g}$
Fluid drag force		$\vec{f}_{f,i}$	$\dfrac{\beta V_{pi}}{1-\varepsilon}\left(\vec{U}-\vec{V}_i\right)$

$$\beta=\begin{cases}\left[150\dfrac{(1-\varepsilon)^2\mu_f}{\varepsilon^2 d_{pi}^2}+1.75\dfrac{\rho_f(1-\varepsilon)\left|\vec{U}-\vec{V}_i\right|}{\varepsilon d_{pi}}\right], & \varepsilon<0.8\\[3mm]\dfrac{3}{4}C_D\dfrac{\rho_f(1-\varepsilon)\left|\vec{U}-\vec{V}_i\right|}{d_{pi}}\varepsilon^{-2.65}, & \varepsilon\geq0.8\end{cases}$$

$$C_D=\begin{cases}\dfrac{24\left[1+0.15\,\mathrm{Re}_{p,i}^{0.687}\right]}{\mathrm{Re}_{p,i}}, & \mathrm{Re}_{p,i}<1000\\[3mm]0.44 & , \mathrm{Re}_{p,i}\geq1000\end{cases}$$

where: $\vec{R}_i=\vec{x}_j-\vec{x}_i,\vec{n}_i=\dfrac{\vec{R}_i}{\left|\vec{R}_i\right|},\vec{V}_{r,ij}=\vec{V}_i-\vec{V}_j$ $\mathrm{Re}_{p,i}=\dfrac{\rho_f d_{pi}\varepsilon\left|\vec{U}-\vec{V}_i\right|}{\mu_f},\vec{F}_{fp}^B=\sum_{i=1}^{i=k_c}\vec{f}_{f,i}/V_c$

Table 2: Computational conditions used in the present simulations

Particle phase		Gas Phase		
Particle	Polyethylene	Fluid		Air
Particle shape	Spherical	CFD cell	Width (m)	3×10^{-3}
Number of Particles	2500 Large 2500 Small		Height (m)	3×10^{-3}
Particle diameter (m)	0.001,0.0008			
Density (kg.m^{-3})	920	Bed geometry	Width (m)	0.06
Spring constant (N.m^{-1})	800		Height (m)	0.24
Sliding friction coefficient	0.3		Thickness (m)	1×10^{-3}
Restitution coefficient	0.9			
Heat capacity (W.kg^{-1}.K^{-1})	2.01×10^3	Viscosity (kg.m^{-1}.s^{-1})		1.85×10^{-5}
Normal tensile strength (Pa)	30×10^6	Bed distributor		Porous Plate
Surface tension (Nm^{-1})	0.0275	U_{mf}(m.s^{-1})		0.187
		Gas velocity (m.s^{-1})		$4U_{mf}$
Time step (s)	5×10^{-7}	Conduction coefficient (W.m^{-1}.K^{-1})		2.9×10^{-2}
		Heat capacity (W.kg^{-1}.K^{-1})		1.8×10^3
		Time step (s)		1×10^{-4}

Figure 1 shows the snapshots of the agglomerating fluidized bed in which the hot gas (110^0 C) was injected to the bed at the superficial gas velocity of 0.75 m.s^{-1}. In this figure, particles are colored according to their temperature. As can be seen in Figure 1, at the beginning of simulation (t = 6 sec.), injecting the hot gas through the distributor only affects the temperature of particles near the distributor. There are hot zones at the vicinity of the distributor as well as at the corner of the bed. According to the viscous flow mechanism (Eqs.(3)-(5)), the probability of solid bridge formation between two particles increases by increasing the contact time and temperature of contacting particles. Therefore, dense regions, in which particles have more contact time and dead zones at the corner of the bed and the distributor zone with high temperature, are introduced as regions in where the possibility of the agglomeration formation is greater. As a result, only particles at the distributor zone have the potential to form the agglomerates and light agglomerates comprised of two or three particles start to form. At this time, the bed is completely fluidized and vigorous bubbles pass through the bed. Rising bubbles in the bed create particle circulation which results in the mixing of particles and increasing the bed temperature, generally. Thus, after elapsing enough time (t = 12 sec.), not only the particles at the vicinity of the distributor, but also the particles at the middle and top of the bed may participate in agglomeration formation. At this time, the bed is gradually transformed into a de-fluidized bed with small bubbles. At the end of simulation (t = 30 sec.), massive agglomerates are gathered in the distributor zone and a de-fluidized layer is formed in this region. This is due to the fact that de-fluidization in this process occurs as a consequence of two different mechanisms: sintering and segregation. Formation of large agglomerates, which have minimum fluidization velocities greater than the gas velocity applied in simulation, leads to accumulation of a large fraction of agglomerations at the bottom of the bed. Thus, segregation promotes the de-fluidization by increasing the contact time of particles. In this situation, small bubbles exist only in the middle or surface of the bed.

Figure 2 shows longitudinal temperature profile of particles and gas at two gas velocities. A steep gradient of the bed temperature can be found near the distributor above which the bed temperature is almost constant. By increasing the inlet gas velocity, the gas affects on the particles at higher levels of the bed due to enhancing the energy content introduced into the bed and increasing the heat transfer coefficient between gas and particles. These results show that the distributor zone is a region with the most possibility of agglomerate formation in the bed and a major fraction of agglomerates form at the distributor zone.

3.2. Macro-Scale studies

According to the model used in this work (Eqs. (3)-(5)), two parameters may affect the strength of the solid bridge in the sintering phenomena: residence time of particles in close proximity and temperature of sintering particles. The residence time in the quiescent zones must be sufficiently long for solid bridge to reach a size in which the formed agglomerates are enough strong to prevent their breakage by the bubble motion. On the other hand, based on the viscous flow mechanism, the solid bridge growth is caused by mass transfer to the contact point of particles. Thus, higher temperature of colliding particles results in formation of stronger solid bridge. Therefore, sintering occurs in the quiescent zones in which relative motions of particles are limited and hot zones in which the temperature of contacting particles are high. It is known that among the operating parameters, such as inlet gas velocity, pressure and inlet gas temperature, the inlet gas temperature directly influences the strength of the solid bridge by affecting on the particles temperature and consequently their residence time. Moreover, the coupled

DEM-CFD is an appropriate tool for particle-level studies such as agglomeration process. Therefore, the effect of inlet gas velocity is investigated in macro and micro scales in the following section.

Figure 3 demonstrates the number of agglomerates versus time at various inlet gas temperatures at t=20 sec. It can be seen from this figure that the number of agglomerates increases with increasing the inlet gas temperature. Because the temperature of colliding particles increases with increasing the inlet gas temperature, the possibility of formation of stronger solid bridge becomes greater. Thus, the number of solid bridges which can sustain versus repulsive forces is increased.

The influence of inlet gas temperature on the mass of agglomerates at t= 20 sec. is shown in Figure 4. According to this figure, the distribution of agglomerates shifts to heavier agglomerates and its tail becomes wider as the inlet temperature is increased from 100 ^{0}C to 120 ^{0}C. Also, Figure 4 demonstrates that there are two peaks at the inlet gas temperature of 130 ^{0}C: one corresponding to the light agglomerates and the other to the massive agglomerates containing more than ten particles. The higher inlet gas temperature increases the temperature of colliding particles. As the rate of material migration to the contact point increases exponentially with temperature of colliding particles, the rate of sintering enhances dramatically at 130 ^{0}C. This situation results in formation of massive agglomerates which form a de-fluidized layer at the distribution region.
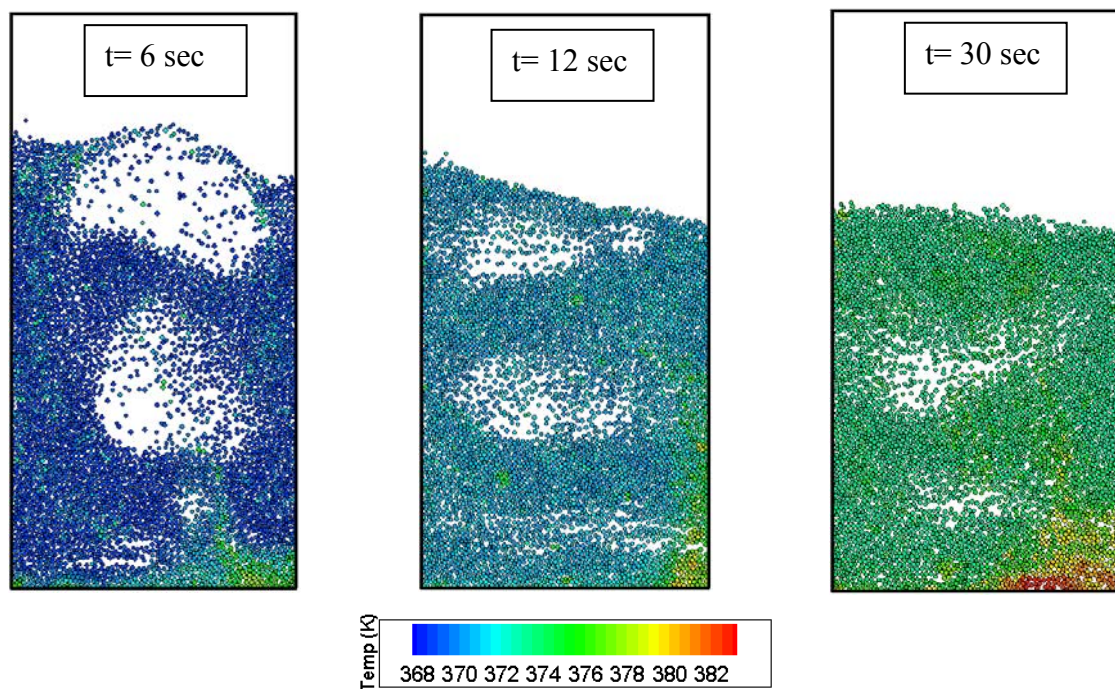

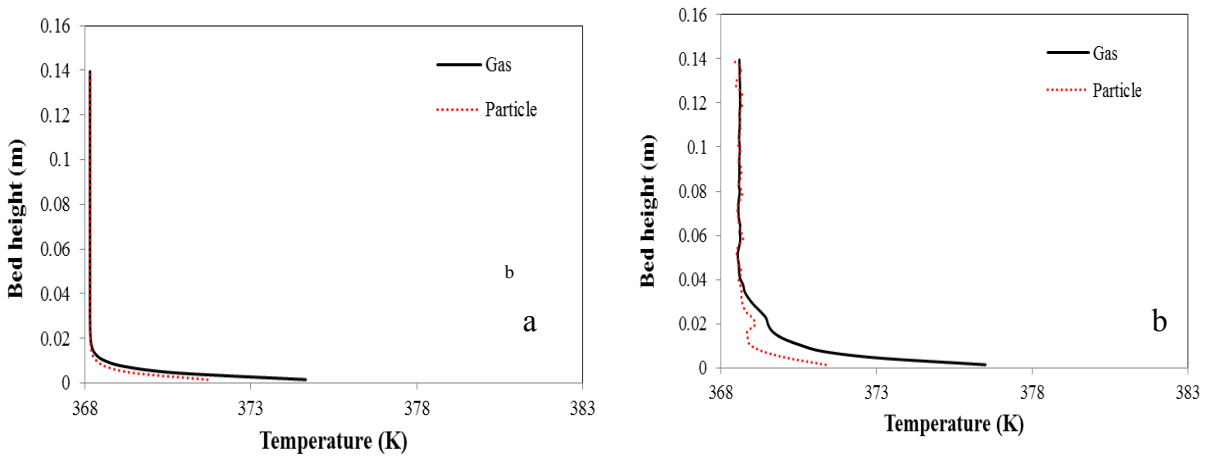**Figure 1: The snapshots of particles temperature during the agglomeration phenomena**

Figure 2: Vertical profile of particles and gas temperature a) U/Umf=2, b) U/Umf=5
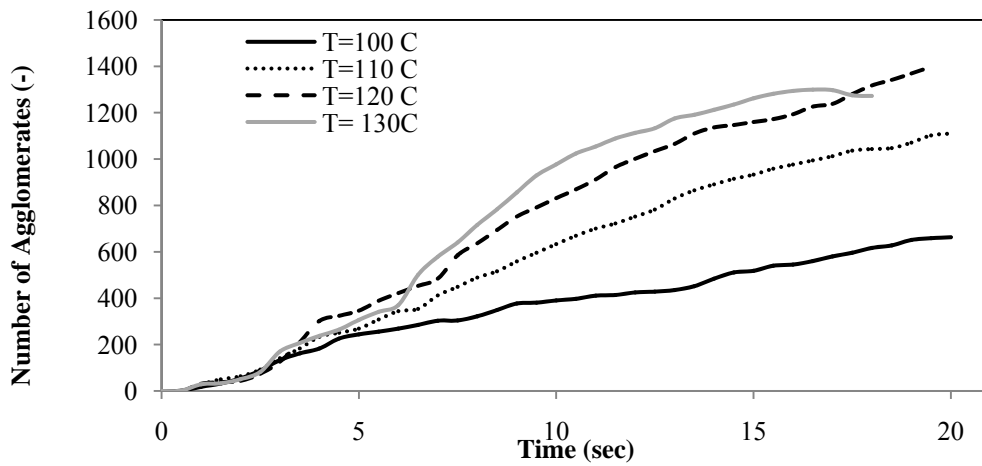

Figure 3: The profiles of number of agglomerates versus time at various inlet gas temperatures
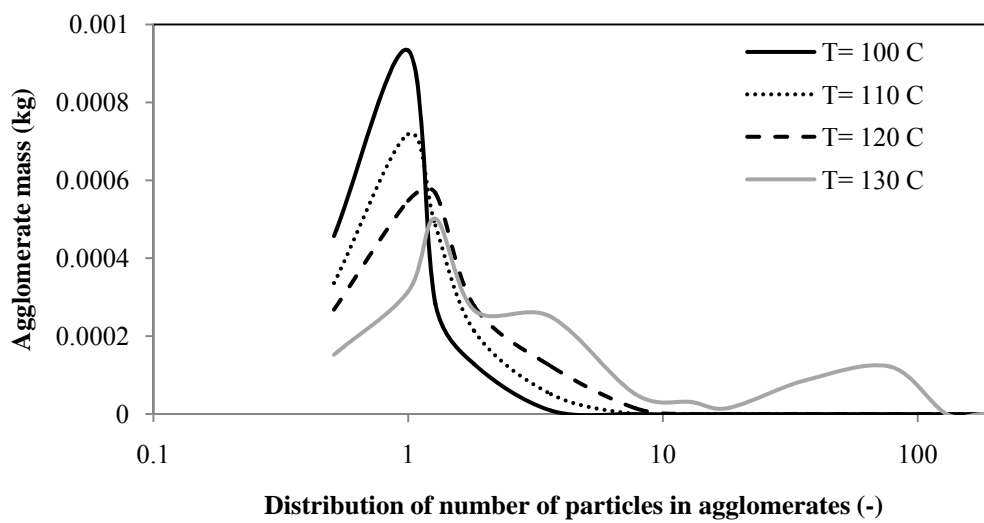

Figure 4: Distribution of mass of agglomerates at different inlet gas temperature
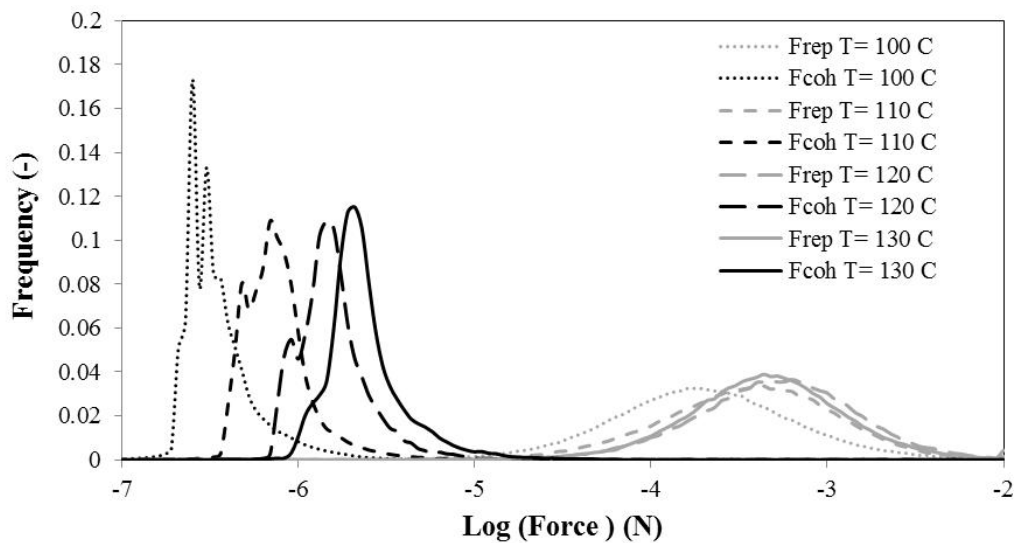
Figure 5: The distributions of cohesion force (curves in left side) and repulsion force (curves in right side) in the logarithmic scale at different inlet gas temperature
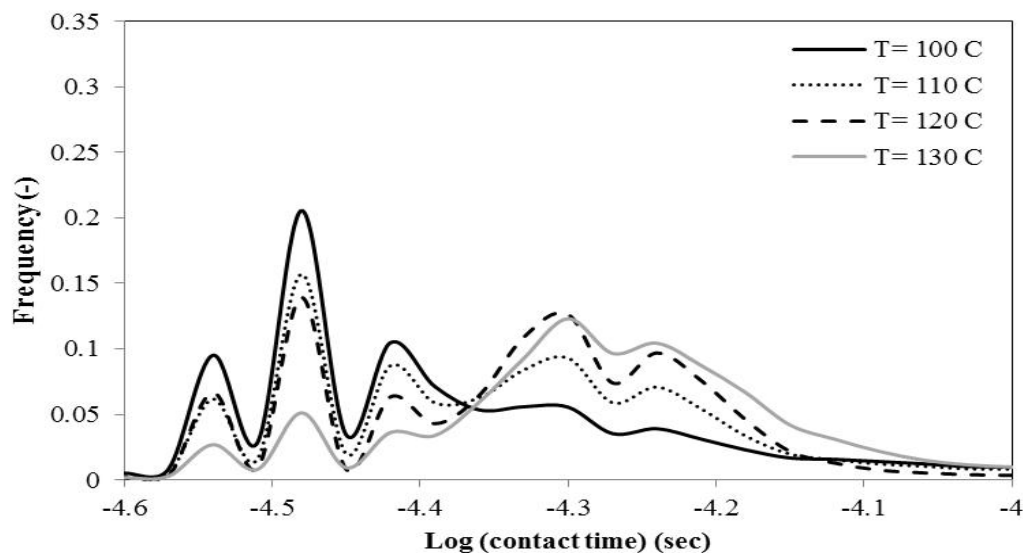

Figure 6: Distribution of particles logarithmic contact time for different gas velocities at t = 15 sec

3.3. Micro-Scale studies

To investigate the cause of these macro-scale studies, it is necessary to focus on micro-scale phenomena and particle-particle interactions. It is known that there exist three phenomena in formation of a permanent solid bridge:

1) The possibility of solid bridge formation between the particles in contact. The lower number of contacts between particles reduces the possibility of solid bridge formation.

2) The possibility of permanent solid bridge formation which is sufficiently strong to resist the breakage forces due to movement of other particles and bubbles. According to the viscose flow mechanism (Eqs. 3-5), the cohesive force (f_{coh}) depends on the temperature of colliding particles and their contact time.

3) The chance of breakage of solid bridge is the last aspect that affects on the permanent solid bridge formation. A high relative velocity of particles before collision enables particles to overcome

the inter-particle cohesive force due to increase in the maximum overlap and repulsion force ($f_{rep,max}$).

Therefore, understanding the microscopic mechanism in terms of contacts time t_{cont}, f_{coh} and $f_{rep,max}$ is vital to truly explore the agglomeration phenomena at high temperatures.

According to the above mentioned concepts, cohesion and repulsion forces affect on the formation of permanent solid bridge between particles in contact. Distributions of cohesion and repulsion forces at various inlet gas temperatures are illustrated in Figure 5. It can be seen from this figure that as the temperature increases, the cohesion force becomes greater while the repulsion force does not change significantly. According to Figure 1, the temperature of particles is increased and in return the cohesion force is enhanced with increasing the inlet gas temperature. On the other hand, the repulsion force between colliding particles does not change considerably. According to the criteria for examination of solid bridge strength described in solid bridge force section, the permanent solid bridge is formed when the cohesion and repulsion forces have the same order of magnitude. Therefore, the amount of overlap between the curves of cohesion and repulsion forces can be a criterion for forming permanent solid bridge. According to Figure 5, the overlap increases with increasing the inlet gas temperature. In fact, the cohesion force grows about two orders of magnitudes while repulsion force does not increase significantly by increasing the temperature from 100 ^{0}C to 130 ^{0}C. Thus, the cohesion force, as a positive factor in sintering, is more sensitive to increase in the inlet gas temperature than the repulsion force, as a negative factor in the formation of agglomerates.

Distribution of the contact time of particles in the logarithmic scale at various inlet gas temperature at $t = 15$ sec. is shown in Figure 6. This figure shows that the contact time between particles increases when the inlet gas temperature is increased. By increasing the inlet gas temperature, the sharp peaks become smaller while the wide part of distribution grows. This is due to this fact that as the temperature is increased, the number of individual particles with smaller contact time decreases and the number of large agglomerates with greater contact time increases. On the other hand, segregation phenomena and reduction in the movement of agglomerates lead to growth of the wide part of the distribution, especially at the highest temperature (130 ^{0}C). As mentioned in Figure 4, massive agglomerates with more than ten particles form in 130 ^{0}C. These massive agglomerates result in a wide distribution at large contact times.

Conclusions

Simulation of an agglomerating fluidized bed was performed by the CFD-DEM technique based on the viscous mechanism. Temperature distributions of gas and particles were obtained by introducing the equation of conservation of energy for both phases. The translational and rotational motions of agglomerates were modeled according to the multi-sphere method. A more realistic simulation of fluidization during the agglomeration process was obtained by taking the rotational motion of agglomerates and distribution of particle temperature into account in comparison to previous works. De-fluidization behavior of the bed was successfully illustrated in terms of mass and size of agglomerates in different inlet gas temperatures. The mechanistic results showed that the repulsive force, as a negative factor in formation of agglomerate, is less sensitive to the inlet gas temperature in comparison with the cohesive force, as a positive factor. By increasing the inlet gas temperature, the contact time is increased. On the other hand, stronger solid bridge is formed between colliding particles due to higher particle temperature at higher inlet gas temperatures. Thus, higher particles temperature and higher contact times of colliding particles in larger agglomerates with restricted

movements promote the agglomeration process and initiate the de- fluidization state in the bed in shorter times.

Nomenclature

C_D	fluid drag coefficient
d_p	particle diameter, m
e	restitution coefficient
E_s	activation energy of surface viscosity, J mol^{-1}
$\vec{f}_{Coh}$	cohesive force between particle i and j, N
$\vec{f}_{Cont,n,ik,j}$	normal contact force between particle i and j or particle k in agglomerate i and particle j, N
$\vec{f}_{Cont,t,i,j}$	tangential contact force between particle i and j or particle k in agglomerate i and particle j, N
$\vec{f}_{f,i}$	particle-fluid interaction force, N
$\vec{f}_{g,i}$	gravitational force of particle i or particle k in agglomerate i N
$\vec{f}_{rep,max}$	max repulsive force of particle i and j or particle k in agglomerate i and particle j, N
g	gravitational acceleration, m s^{-2}
I_i	moment of inertia of particle or agglomerate i, kg m^2
k_i	number of contacting particle j with particle i or particles k in agglomerate i
k_n	normal spring coefficient, N m^{-1}
k_t	tangential spring coefficient, N m^{-1}
m_i	mass of particle and agglomerate i, kg
$\vec{n}$	unit vector
r	reduce radius of colliding particles, m
$\overline{R}$	gas constant, J mol^{-1}K^{-1}
$\vec{R}_{i,j}$	The vector from particle i to particle j, m

Re	reynolds number
t	time, s
t_{con}	contact time, s
$t_{con,0}$	contact time in previous time step, s
$_{ij}$	torque, N m
T	maximum temperature of colliding particles, K
U	fluid velocity, ms^{-1}
U_{mf}	minimum fluidization velocity, ms^{-1}
V_c	cell volume, m^3
V_i	velocity of particle and agglomerate i, m s^{-1}
V_p	particle volume, m^3
$x_{s.b.}$	solid bridge radius, m

Greek symbol

β	inter-phase momentum transfer coefficient, kg m-3s-1
γ_p	surface tension, Nm^{-1}
δ	deformation coefficient, m
ε	Porosity
η	damping coefficient
μ	friction coefficient
μ_f	fluid viscosity, kg m^{-1} s^{-2}
μ_p	particle viscosity, kg m^{-1} s^{-2}
μ_0	pre exponential factor, kg m^{-1} s^{-2}
ρ_f	fluid density, kg m^{-3}
ρ_p	particle density, kg m^{-3}
σ	normal tensile strength, Pa
ω_i	angular velocity of particle i or particle k in agglomerate i, s^{-1}

Subscript

g	Gas
p	Particle
s.b.	solid bridge

References:

1- Anderson, T.B. and Jackson, R.A. (1967). "Fluid mechanical description of fluidized beds: Equations of motion." *Ind. Eng. Chem. Fund.*, Vol. 6, pp. 527-539..

2- Cundall, P.A. and Strack, O.D.L. (1979). "A discrete numerical model for granular assemblies." *Geo technique*, Vol. 29, pp. 47–65.

3- Deen, N.G., Annaland, Van Sint M., Van der Hoef, M.A. and Kuipers, J.A.M. (2007). "Review of discrete particle modeling of fluidized beds." *Chem. Eng. Sci.*, Vol. 62, pp. 28-44.

4- Mikami, T., Kamiya, H. and Horio,M. (1998). "Numerical simulation of cohesive powder behavior in a fluidized bed." *Chem. Eng. Sci.*, Vol. 53 No. 10, pp.1927-1940.

5- Iwadate, Y. and Horio, M. (1998). "Prediction of agglomerate sizes in bubbling fluidized beds of group C powder." *Powder Technol.*, Vol. 100, pp. 223-236.

6- Li, Sh., Marshall, J. S., Liu, G. and Yao, Q. (2013) "Adhesive particulate flow: The discrete-element method and its application in energy and environmental engineering." *Progr. Energ. Combust. Sci.*, Vol. 37, pp. 633-668.

7- Kuwagi, K., Mikami, T. and Horio, M. (2000). "Numerical simulation of metallic solid bridge particles in a fluidized bed at high temperature." *Powder Technol.*, Vol. 109, pp.27-40.

8- Mansourpour, Z., Mostoufi, N. and Sotoudeh-Gharebagh, R. (2013). "A mechanistic study of agglomeration in fluidized beds at elevated pressures." *The Canadian J. Chem. Eng.*, Vol. 91, pp. 560-569.

9- Mansourpour, Z., Mostoufi, N. and Sotoudeh-Gharebagh, R. (2014). "Investigating agglomeration phenomena in an air-polyethylene fluidized bed using DEM–CFD approach." *Chem. Eng. Res. Des.*, Vol. 92, pp. 102-118.

10- Mansourpour, Z., Karimi, S. Zarghami, R., Mostoufi, N. and Sotoudeh-Gharebagh, R. (2010). "Insights in hydrodynamics of bubbling fluidized beds at elevated pressure by DEM–CFD approach." *Particuology*, Vol. 8, pp. 404-414.

11- Kruggel-Emden, H., Rickelt, S. Wirtz, S. and Scherer, V. (2008). "A study on the validity of the multi-sphere discrete element method." *Powder Technol.*, Vol. 188, pp. 153-165.

12- Seville, J.P.K., Willett, C.D. and Knight, P.C. (2000). "Interparticle forces in fluidization: a review." *Powder Technol.*, Vol. 113, pp. 261-268.

13- Seville, J.P.K., Silomon-Pflug, H. and Knight, P.C. (1998). "Modeling of sintering in high temperature gas fluidization." *Powder Technol.*, Vol. 97, pp.160-169.